Pamukkale Üniversitesi Mühendislik Bilimleri Dergisi
Pamukkale University Journal of Engineering Sciences

Investigation of the effects of precision-casting waste sands on the thermal shock resistance properties of fire clay refractory materials

Hassas döküm atık kumlarının ateş kili refrakter malzemelerin termal şok direnci özelliklerine etkilerinin araştırılması

Veysel Murat BOSTANCI[1], Tuba BAHTLI[2]*

[1]Necmettin Erbakan University, Faculty of Engineering, Department of Basic Sciences, Konya, Türkiye.
veyselmurat.bostanci@erbakan.edu.tr
[2]Necmettin Erbakan University, Faculty of Engineering, Department of Metallurgical And Material Engineering, Konya, Türkiye.
taksoy@erbakan.edu.tr

Received/Geliş Tarihi: 21.05.2024 Revision/Düzeltme Tarihi: 12.11.2024 doi: 10.5505/pajes.2024.82496
Accepted/Kabul Tarihi: 16.12.2024 Research Article/Araştırma Makalesi

Abstract

Precision-casting is a casting process that minimizes porosity and has the power to produce exact shapes and sizes of parts. In the metal part production sector, precision-casting is the closest casting form to the final version of the part. Using single-use aluminosilicate molds in casting operations causes a storage problem after precision-casting, which adds to the expanding waste problem. Moreover, the disposal of this waste without recycling poses environmental concerns. Interestingly, the waste contains zircon minerals, which are well-known for improving refractories' mechanical, thermal, and corrosion-resistant qualities. The aim of this study is to produce fireclay refractory bricks that have decreased manufacturing costs, increased mechanical and thermal properties, and are improved by the addition of precision-casting sand. Density and open porosity were determined using the Archimedes principle. Cold crushing strength was tested according to ASTM-C133, and three-point bending tests were performed according to ASTM-C1161-90 standards. For thermal shock resistance, samples were heated to 1000°C for 30 minutes and then quenched in water. Finally, microstructure analyses were conducted using a scanning electron microscope (SEM). Compared to the additive-free fireclay refractory, samples containing X2, Y2, and Z1 precision-casting waste sand (PCWS) showed increases in 3-point bending strength by 27%, 10%, and 5%, respectively, after undergoing thermal shock testing. Similarly, with the addition of PCWS, X2 and Y2 samples exhibited increases of 17% and 33% in cold crushing strength (CCS) values.

Keywords: Thermal Shock, waste, mechanical properties, refractory, precision-casting, fireclay.

Öz

Hassas döküm, gözenekliliği en aza indiren ve parçaların tam şekil ve boyutlarını üretebilme gücüne sahip bir döküm işlemidir. Hassas döküm, metal parça imalat endüstrisinde nihai parça versiyonuna en yakın döküm şeklidir. Döküm işlemlerinde tek kullanımlık alüminasilikat esaslı kalıpların kullanımı, hassas döküm sonrası bir depolama sorununa yol açmakta ve giderek artan bir atık sorununa katkıda bulunmaktadır. Dahası, bu atığın geri dönüşüm olmadan bertaraf edilmesi çevresel endişelere yol açmaktadır. Özellikle, atık zirkon minerali içermekte ve bu mineraller refrakterlerin mekanik, termal ve korozyon özelliklerini arttırmakla bilinmektedir. Bu araştırma, maliyetleri düşürülmüş, mekanik ve termal özellikleri arttırılmış ve hassas döküm kumu eklenerek iyileştirilmiş ateş tuğlası refrakterler oluşturmayı amaçlamaktadır. Yoğunluk ve açık gözeneklilik, Arşimet prensibiyle belirlenmiştir. ASTM-C133 standardına göre soğuk basma mukavemeti, ASTM-C1161-90 standardına göre üç nokta eğme testleri gerçekleştirilmiştir. Isıl şok dayanımı için numuneler, 1000°C'de 30 dakika bekletildikten sonra suya daldırılarak test edilmiştir. Son olarak, mikroyapı analizleri taramalı elektron mikroskobu (SEM) ile yapılmıştır. Katkısız şamot refrakterine kıyasla, X2, Y2 ve Z1 hassas döküm atık kumu (PCWS) eklenen numunelerde, termal şok testi sonrasında 3 nokta eğilme mukavemeti sırasıyla %27, %10 ve %5 oranında artmıştır. Benzer şekilde, PCWS ilavesiyle X2 ve Y2 numunelerinde soğuk ezme mukavemeti (CCS) değerlerinde sırasıyla %17 ve %33 oranında artış gözlemlenmiştir.

Anahtar Kelimeler: Termal şok, atık, mekanik özellikler, refrakter, hassas döküm, şamot.

1 Introduction

The basic lining materials for furnaces used in high-temperature operations like melting glass, producing steel, and making cement are called refractory materials [1],[2]. Throughout their service lives, these materials are continuously subjected to high temperatures and thermal shocks, which cause internal strains and thermomechanical failures [3], [4]. Considering the requirements for service safety and durability, the thermal-mechanical damage characteristics of these materials are of great importance [2],[3].

Refractories are typically produced from combinations or individual materials such as alumina, silica, magnesia, zirconia, and chrome [5],[6]. The alumina-silica refractory group, notably a widely used subcategory, is classified into chamotte refractories and high-alumina refractories based on their physical and chemical structures [7]. Chamotte refractories, made from natural clay (rich in silica), can withstand temperatures above a pyrometric cone equivalent (PCE) value of 19 without breaking, deforming, cracking, softening, or melting. These refractories are typically composed of kaolinite clay minerals ($Al_2O_3 \cdot 2SiO_2 \cdot 2H_2O$), and the typical composition of fireclay bricks is 78% SiO_2 and 44% Al_2O_3. Refractories in this class are widely used in various industries, including energy production high furnaces, chimney linings, boilers, glass tank furnaces, and pottery kilns. Additionally, chamotte is used in the production of cast refractories such as nozzles, sleeves, stoppers, and tuyeres [5],[6],[8].

*Corresponding author/Yazışılan Yazar

Chamotte plays a significant role in the construction sector as insulation and building materials due to its high thermal shock resistance, refractoriness, and corrosion resistance properties [9]. Chamotte, which is composed of 18–44% alumina and 50–60% silica, is used as an insulating material to resist high temperatures. Among refractory materials chamotte, magnesia, alumina, chrome, and zirconia are notably the most important ones [10]. Laboratory crucibles/regulators, furnace linings, and insulation beneath hot surfaces are applications for chamotte refractory. Given the wide range of applications for chamotte, it holds great importance for ceramic product manufacturers.

Furthermore, adding alumina abrasive waste to chamotte bricks is noted to enhance the percentages of silicon dioxide (SiO_2) and aluminum oxide (Al_2O_3). This improvement is suggested to lead to an increase in the density and mechanical properties of chamotte bricks. Some researchers have demonstrated that the incorporation of zircon particles as a reinforcement in low-cement castables not only improves mechanical properties but also enhances thermal properties [11].

In furnaces used in steel, glass, ceramics, and other high-temperature industries, Al_2O_3–SiO_2 refractories are commonly utilized [12], [13], [14]. Among the traditional shaping methods for formed refractories are techniques such as dry pressing, gel casting, and hot pressing [15], [16], [17]. These methods enable the production of refractory materials in specialized shapes used in various industries.

The expanding global economy and intense industrial rivalry are causing significant environmental harm and leading to the unsustainable depletion of natural resources. To transition towards a more environmentally friendly and sustainable economy, it is imperative to adopt production models with minimal ecological footprints. Precision-casting, also known as lost wax casting, stands out as one of the predominant methods for manufacturing intricate metal components. In this intricate process, liquid metal is poured into a disposable ceramic mold and allowed to solidify. Subsequently, the ceramic shell molds are fractured, and the cast metals are retrieved [18]. Consequently, the precision-casting sector annually produces millions of tons of waste in the form of refractory precision-casting shell material [19].

These ceramic shell molds commonly consist of valuable refractory materials such as silica, mullite, and zircon. However, the strict demands of the casting process render waste shell molds non-recyclable and non-reusable. As a result, these discarded ceramic shell molds typically find their way to landfills. Hence, there is a strong desire to develop an economically viable recycling process that can add value to this waste [20].

Special qualities of zircon include resistance to molten metal penetration, great erosion resistance, superior thermal shock resistance, and dimensional stability. As a result, it is favored over other refractories in the ceramic and metallurgical industries [21].

Studies on the recycling of precision-casting waste indicate the potential for these materials to be repurposed as raw materials in ceramic and structural applications. In Sevnur Özdemir's thesis, "Reuse of Investment Casting Mold Sands in the Ceramic Industry," the use of casting mold waste in ceramics was examined, aiming to reduce its environmental impact by repurposing it in ceramic components [22]. Similarly, Yusuf Erdem's study investigated the effects of substituting clay and kaolin with different types of investment casting waste sand in porcelain tile production, evaluating how these casting sands contribute to the production process while also promoting raw material recovery and environmental sustainability [23].

Another significant study in this field is Celal Avcıoğlu's thesis, "Reuse of Spent Investment Casting Foundry Sands in the Production of Structural Ceramics." Avcıoğlu aimed to reduce the environmental impact of investment casting shell waste by using it in high-performance ceramic composites. His study developed mullite-zirconia and cordierite-based composites, both of which exhibited excellent strength and radiation shielding properties [24].

Research indicates that these ceramic shell wastes can be effectively recycled to recover valuable refractory aggregates, such as zircon sand, which can be reused in the production of new casting shells [25]. This recycling process not only reduces waste but also minimizes the demand for virgin materials, contributing to a more sustainable production cycle. Additionally, recycling these materials leads to cost savings in the production process by reducing the need for new raw materials [26].

This study investigates how waste foundry sands containing zircon in their composition affect the mechanical properties of chamotte refractory bricks after thermal shock.

2 Materials and methods

Refractory materials produced using bauxite and chamotte were prepared for testing, based on a composition determined by utilizing different precision-casting waste sands. The XRF analysis results of the wastes are shown in Table 1, and the composition ratios are presented in Table 2.

Table 1. XRF analysis results

	X (AISI 4140)	Y (AISI 1050)	Z (AISI 2083)	Chamotte 1-3mm	Chamotte 0-1mm	Chamotte Powder	Bauxite 1-3mm
Al_2O_3	22,82	27,65	25,14	33,67	28,53	33,63	71,81
SiO_2	58,03	59,89	66,63	61,48	66,82	59,96	22,99
Fe_2O_3	1,61	1,63	1,43	1,66	1,54	2,46	2,09
TiO_2	2,27	2,53	2,48	2,84	2,52	2,99	2,80
CaO	0,30	0,26	0,41	0,35	0,59	0,96	0,31
ZrO_2	14,74	7,92	3,77	0,00	0,00	0,00	0,00
Others	0,23	0,12	0,14	0,00	0,00	0,00	0,00

The XRF analysis of the precision-casting waste sand (PCSW) (Table 1) shows that the structure was based on Al_2O_3, SiO_2 and ZrO_2.

Table 2. Composition of the products to be produced

	Chamotte 1-3mm (%)	Chamotte 0-1mm (%)	Chamotte Powder (%)	Bauxite 1-3mm (%)	Precision casting waste sand powder (%)	Binding Clay powder (%)
R	20	15	20	35	0	10
X1	20	15	15	35	5	10
X2	20	15	10	35	10	10
X3	20	15	0	35	20	10
Y1	20	15	15	35	5	10
Y2	20	15	10	35	10	10
Y3	20	15	0	35	20	10
Z1	20	15	15	35	5	10
Z2	20	15	10	35	10	10
Z3	20	15	0	35	20	10

For density and pore determination, the samples were immersed in water at room temperature for 24 hours. The calculations used for the density and percentage of open porosity tests conducted through the Archimedes principle (Figure 1) are presented in equations 1 and 2.

Figure 1. Archimedes principle

The samples were placed in the apparatus and weighed on a precision balance, determining their weights in water (W_b). Subsequently, the samples, after being removed from the water, were wiped with a paper towel to remove surface water, and their wet weights were determined using a precision balance (W_c). In the final step, after drying the samples in an oven, their dry weights were measured using a precision balance (W_a). The visible porosity (%) and bulk density values were calculated using Equation 1 and Equation 2 data, as per the British Standard [27].

$$\text{Porosity (\%)} = [(W_c-W_a)/(W_c-W_b)] *100 \quad (1)$$

$$\text{Bulk density} = [d_{water}*W_a/(W_c-W_b)] \quad (2)$$

Tests were conducted according to ASTM-C133 standards for cold crushing strength (Figure 2a). The strength values were calculated by dividing the maximum pressure the material could withstand by the cross-sectional area. Three-point bending tests were performed on a Shimadzu AGS-X device by ASTM-C1161-90 standards. Samples with dimensions of 25mm x 25mm x 150mm were subjected to the three-point bending test (Figure 2b), and strength and toughness values were calculated based on the obtained data.

(a) (b)

Figure 2. a) Cold crushing strength and b) three-point bending test

For the thermal shock test (Figure 3), samples with dimensions of 5cm³ and 25mm x 25mm x 150mm were subjected to a temperature of 1000°C for 30 minutes, followed by immersion in water at room temperature for testing. After the tests, the dried materials were subjected to CCS and three-point bending tests, and the obtained data were processed, and the results were shared.

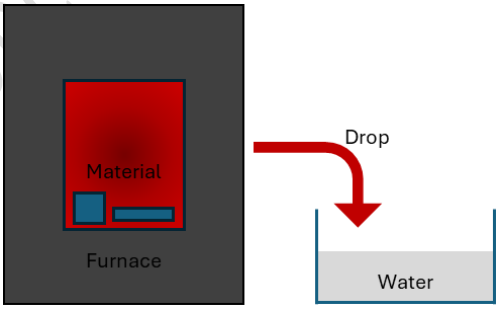

Figure 3. Thermal shock test

Microstructure analyses were conducted after physical and mechanical tests. Following the cutting, mounting, grinding, and polishing stages, microstructure analyses were performed using a Hitachi-SU 1510 scanning electron microscope (SEM) at the Necmettin Erbakan University Science and Technology Research and Application Center (BITAM). Additionally, fracture surface analyses were conducted on the same device.

3 Results and discussion

Figure 4 illustrates the percentages of open porosity and density values for the produced fireclay refractory materials. The density of refractory types X1, X2, Y1, Y2, and Z1 were higher than that of reference material. However, when the additive content goes beyond a certain threshold, the density decreases compared to the additive-free material.

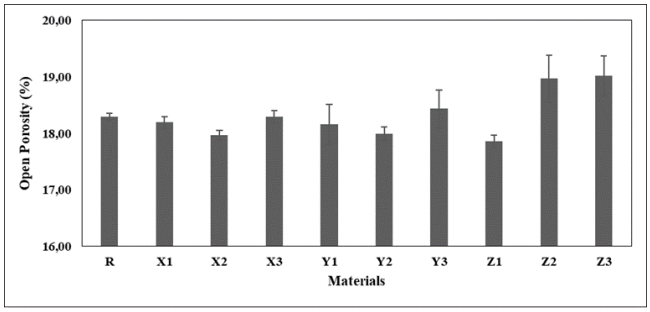

(a)

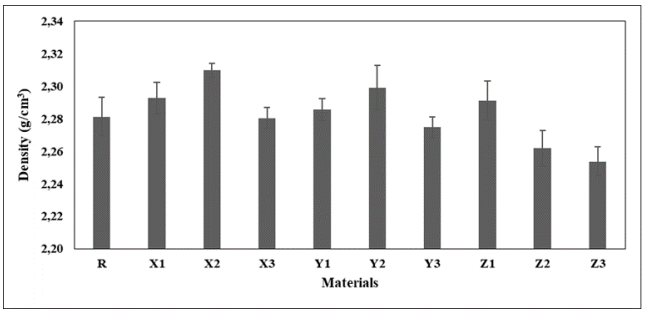

(b)

Figure 4. The values of the produced fireclay refractory materials; a) % open porosity and b) density

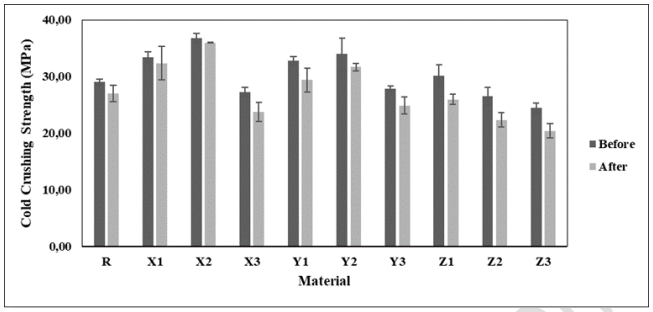

(a)

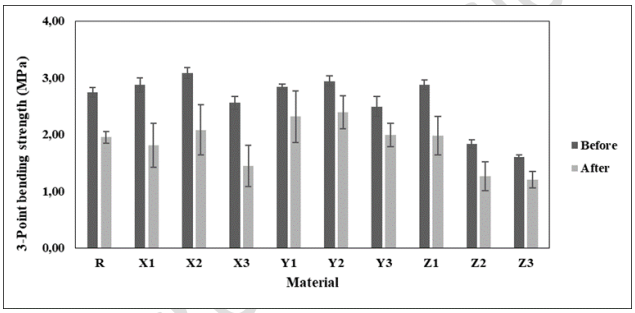

(b)

Figure 5. Before and after thermal shock, a) Cold Crushing Strength (CCS) and b) 3-Point Bending Test results

The incorporation of zircon into the refractory mix contributes to increased density and decreased porosity. This effect is pivotal in enhancing the mechanical properties of material, as highlighted by Aksel [28]. The elevated density and improved thermal characteristics attributed to zircon are reasoned by its inherent density (d_{zircon}: 4.7 g/cm^3), as previously noted by Ceylantekin and Aksel [29], Meng et al. [30] and Xiang et al [31].

An observable outcome of increasing the additive quantity is the rise in microcracks and pores. Furthermore, due to disparate sintering behaviors, it is plausible that the delicate bonds established at the interface between the additive and refractory grains lead to density reduction. This understanding aligns with the findings of Bahtli and Bostanci [32].

CCS values, 3-point flexural strength (Figure 5), and toughness (Figure 6) values of fireclay refractory compositions mechanically tested before and after thermal shock tests are given. For the strength and toughness values determined by the 3-point bending test with CCS, results like the mechanical test results were observed before the thermal shock tests. In general, it is seen that the mechanical properties of all compositions decrease after thermal shock. It is thought that the strength values of pre-existing and newly formed cracks after thermal shock decrease.

The materials coded as X2, Y2, and Z1 enhanced the mechanical properties of chamotte refractories compared to those without additives. Cold crushing strength (CCS) increased by 26%, 17%, and 3% for X2, Y2, and Z1, respectively. Three-point bending strength improved by 12%, 6%, and 4%, while toughness rose by 32%, 30%, and 6% for these additives. After thermal shock testing, CCS showed a 33% and 17% increase with X2 and Y2, respectively. Similarly, three-point bending strength increased by 27%, 10%, and 5% with X2, Y2, and Z1.

Scholarly sources have confirmed the enhanced corrosion resistance, strength, and toughness exhibited by zirconia-mullite composites compared to pure mullite, granting these materials a prominent role in ceramics, especially in critical applications such as glass furnace linings [33]. Pure mullite, consisting of 72-78% Al_2O_3 and 22-28% SiO_2, is known for its high-temperature resistance and thermal shock durability, making it suitable for cost-effective applications. However, zirconia-reinforced mullite composites offer additional advantages, including improved fracture toughness, wear resistance, and thermal stability, allowing them to perform exceptionally in more demanding environments [33], [34]. Moreover, composites that incorporate alumina and zirconia exhibit enhanced strength, toughness, and thermal shock resistance, highlighting their value in advanced ceramic applications [34], [35]

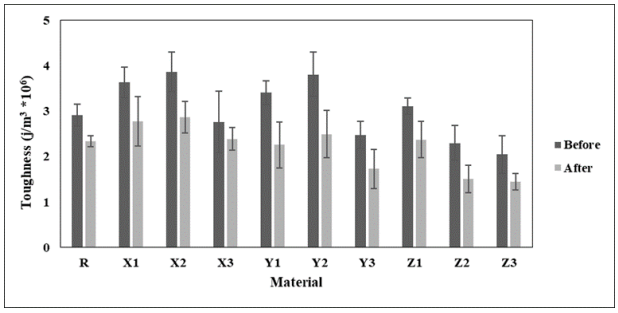

Figure 6. Toughness values of refractories before and after thermal shock

When the toughness values before and after thermal shock were examined, it was observed that the density and strength values increased with the addition of zircon, especially for the fireclay refractories produced with the X1, X2, Y1, Y2 and Z1.

When the results were examined, it was found that the increase in bond strength positively affected the mechanical properties. However, the increase in waste input led to a reduction in bond strength, which, along with the increase in pores and microcracks, was thought to cause a decrease in mechanical properties [36]. When we evaluated the PCWS additions in themselves, it was concluded that higher physical and mechanical properties were obtained with the increase of zircon content.

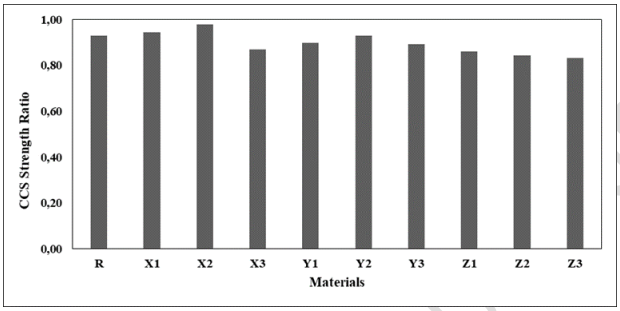

(a)

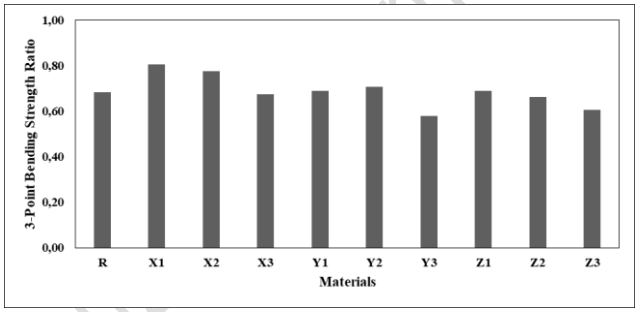

(b)

Figure 7. Strength ratios of refractories for a) Cold Crushing Strength (CCS) and b) 3-point bending

After the cold crushing strength test, it was observed that the strength ratios were generally close to the value of the pure material (Figure 7a). It was observed that the rate was slightly higher in the material with the code X, which has the highest amount of zirconia, compared to the material without additives. It is thought that the fractures after thermal shock have a higher strength ratio than the additive because they are intra- and inter-granular. It is thought that the reason for the high value of those with waste inputs is due to the transformation in the type of fracture after thermal shock [37].

When the 3-point bending strength ratio was examined, the ones with 20% additives were close to the value without additives, while those with 5% and 10% additives were generally slightly higher than those without additives (Figure 7b). The best ratio was seen in the material coded X with the highest amount of zirconia (Table 1). It has been observed that the zircon content is effective in both toughness and thermal shock resistance, as supported by previous findings on composites incorporating alumina and zirconia, which demonstrate enhanced strength, toughness, and thermal shock resistance [34], [35].

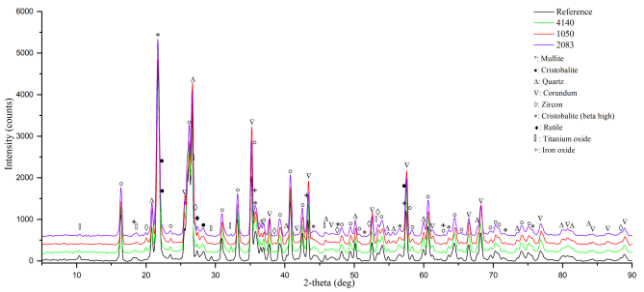

Figure 8. The XRD analysis results

Upon examination of the XRD analysis results (Figure 8), it was determined that Al2O3 and SiO2 phases predominated within the structure. The analysis revealed the presence of various crystalline phases, including mullite (3Al2O3.2SiO2), cristobalite (SiO2), quartz (SiO2), corundum (Al2O3), zircon (ZrSiO4), beta cristobalite (β-SiO2), iron oxide (Fe2O3), and rutile (TiO2).

Mullite forms in all alumina-silica refractory materials heated to sufficiently high temperatures [28]. At temperatures below 1300°C, alumina is largely inert, with primary mullite as the dominant reaction product. However, when the temperature exceeds 1400°C, the formation of secondary mullite begins, followed by subsequent precipitations [38], [39].

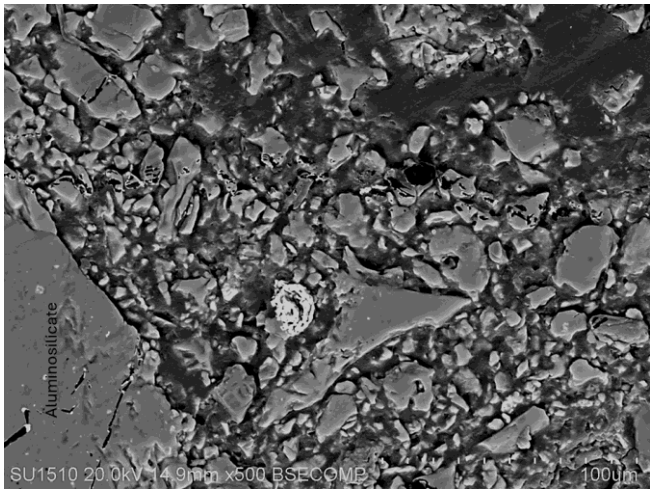

Figure 9. Microstructure image of the reference material

Upon examination of the SEM analyses, it was observed that Figure 9 corresponds to the reference material, with the gray grains identified as aluminosilicate particles derived from the raw material, while the black areas represent pores. In Figure 10, it was noted that, in addition to the aluminosilicate grains and pores, zircon mineral is represented in white. Furthermore, the mapping analyses reveal the elemental distribution within the structure.

In the microstructure analysis of the reference material, the presence of large aluminosilicate grains was detected in the structure, and it was thought that this condition had an impact on both physical and mechanical properties.

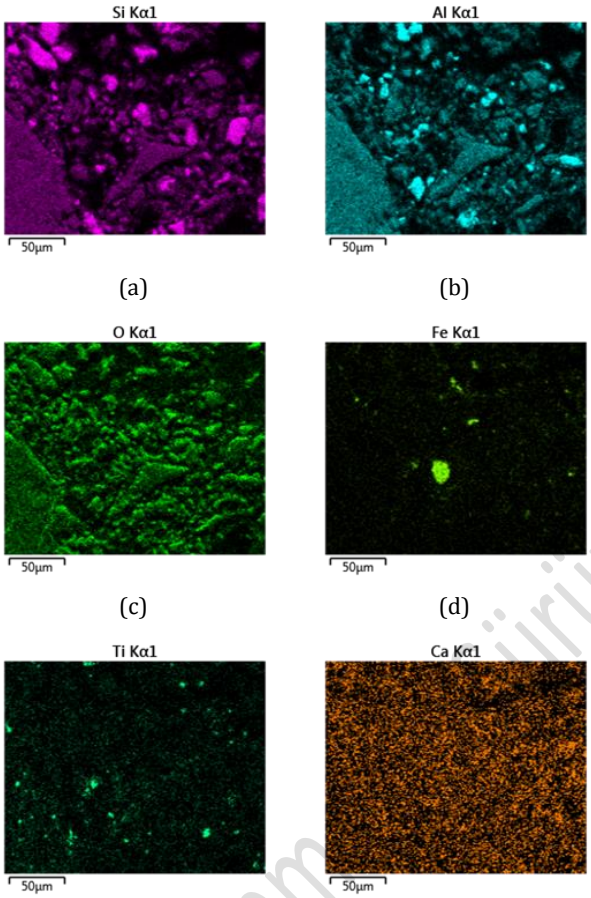

Figure 10. Mapping analysis of the reference material a) Si, b) Al, c) O, d) Fe, e) Ti and f) Ca

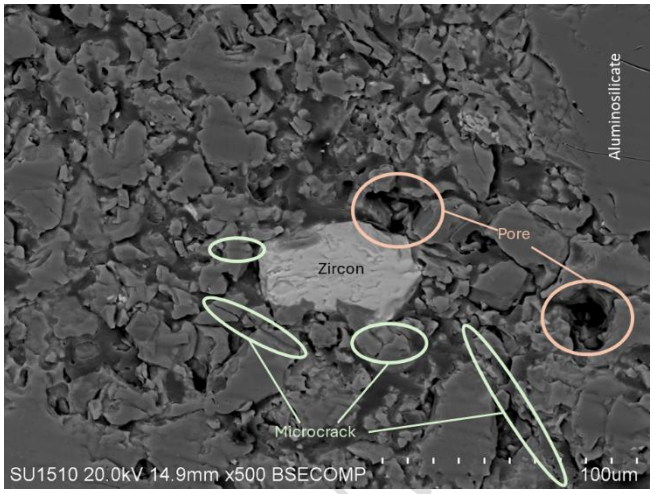

Figure 11. Microstructure image of the X2 material

The addition of X at a rate of 10% resulted in a decrease in the size of aluminosilicate grains and an increased structural density. Moreover, a limited number of short microcracks were observed in the structure, and it was believed that these microcracks, together with zircon grains, contributed to increase toughness (Figure 11) [40]. The formation of microcracks, attributed to the mismatch in thermal expansion coefficients (αmullite = ~4.5-5.5 x 10^{-6} K, αt-ZrO_2 = ~9 x 10^{-6}K) [41], is also considered to support the improvement in toughness [42]. Additionally, mapping analyses illustrate the elemental distribution within the structure (Figure 12).

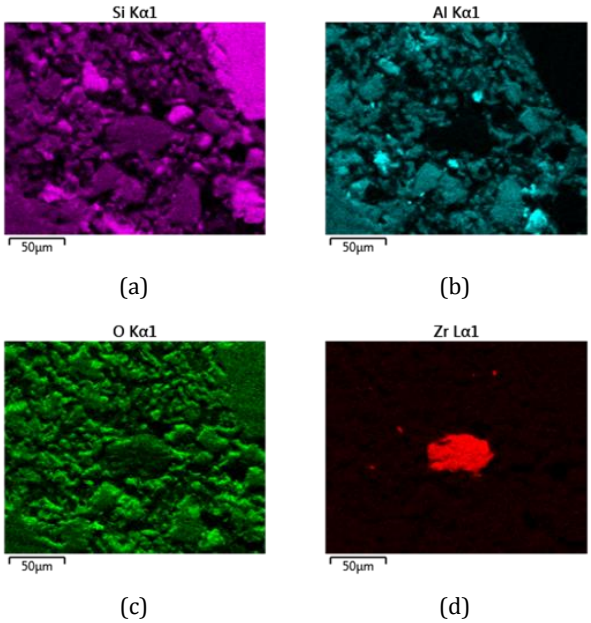

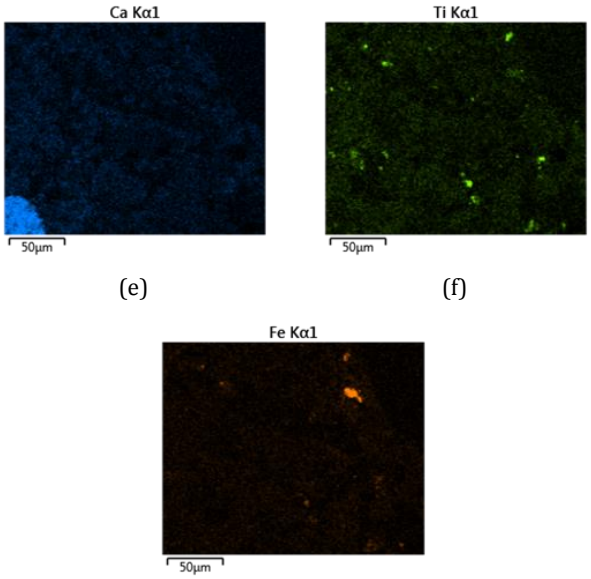

Figure 12. Mapping analysis of the X2 material a) Si, b) Al, c) O, d) Zr, e) Ca, f) Ti and g) Fe

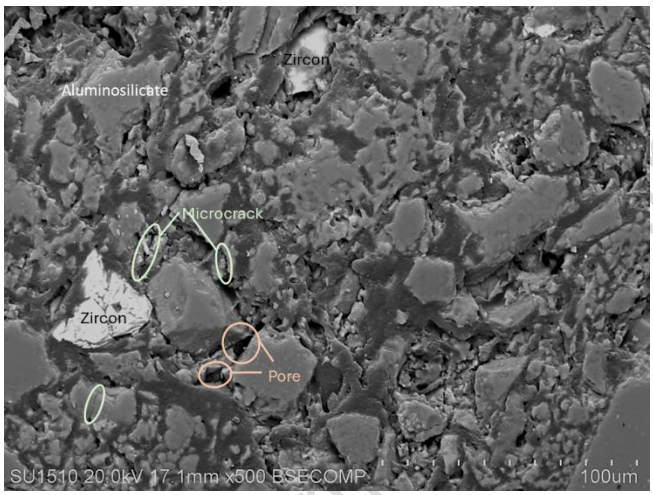

Figure 13. Microstructure image of the Y2 material

Upon examination of the Figure 13, it has been determined that the material consists of smaller grains compared to the pristine material. This situation indicates that the smaller grain size, along with the presence of zircon, microcracks, and pores, contributes to increased toughness. Therefore, it was believed that the material exhibits better mechanical properties compared to the reference material. Additionally, mapping analyses also show elemental distribution within the structure (Figure 14).

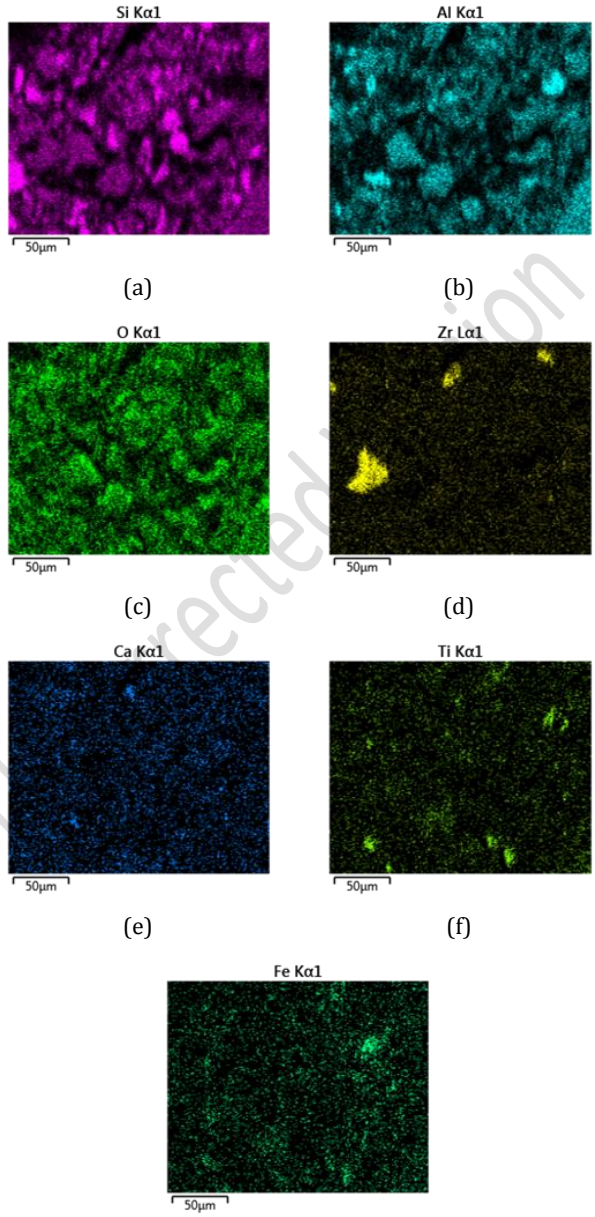

Figure 14. Mapping analysis of the Y2 material a) Si, b) Al, c) O, d) Zr, e) Ca, f) Ti and g) Fe

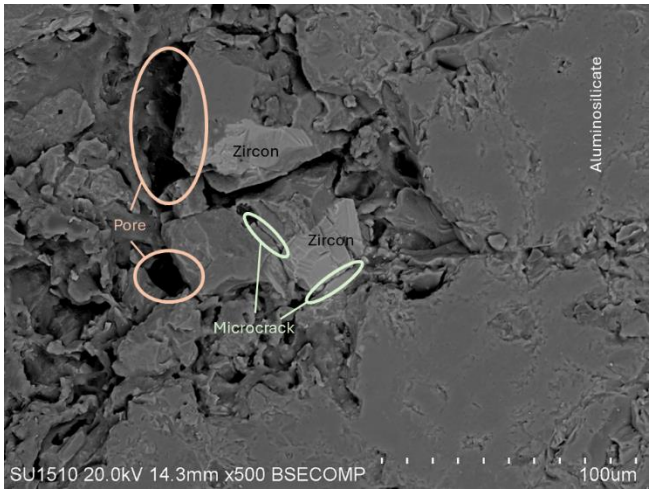

Figure 15. Microstructure image of the Z1 material

Upon examination of the microstructure of the material coded as Z1 (Figure 15), it has been observed that larger grains and deep cracks are present. Additionally, a decrease in mechanical properties has been identified due to the high level of porosity. Additionally, mapping analyses also show the elemental distribution within the structure (Figure 16).

The average grain sizes of aluminosilicate particles in the reference material and in chamotte refractory materials containing X2, Y2, and Z1 PCWS were determined using Image-J software as approximately 55 µm, 32 µm, 35 µm, and 54 µm, respectively. The presence of smaller particles contributes to reduced porosity, and fine waste particles may accelerate the sintering of chamotte refractories, potentially enhancing their mechanical and physical properties. Due to the presence of zircon, the samples with smaller particle sizes exhibit improved toughness attributed to densification, as well as the formation of microcracks and pores that contribute to increased toughness. Consequently, these samples display superior mechanical properties compared to the reference material. Among the samples, Z1 was observed to have larger grains compared to those with X and Y additives, and this larger grain size is associated with lower mechanical properties.

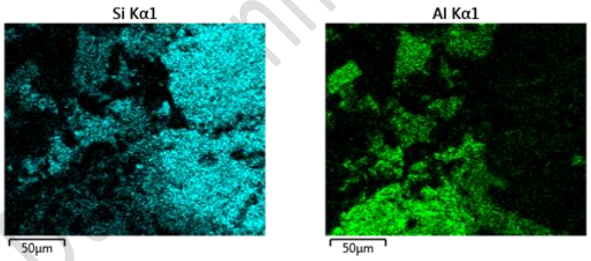

(a) (b)

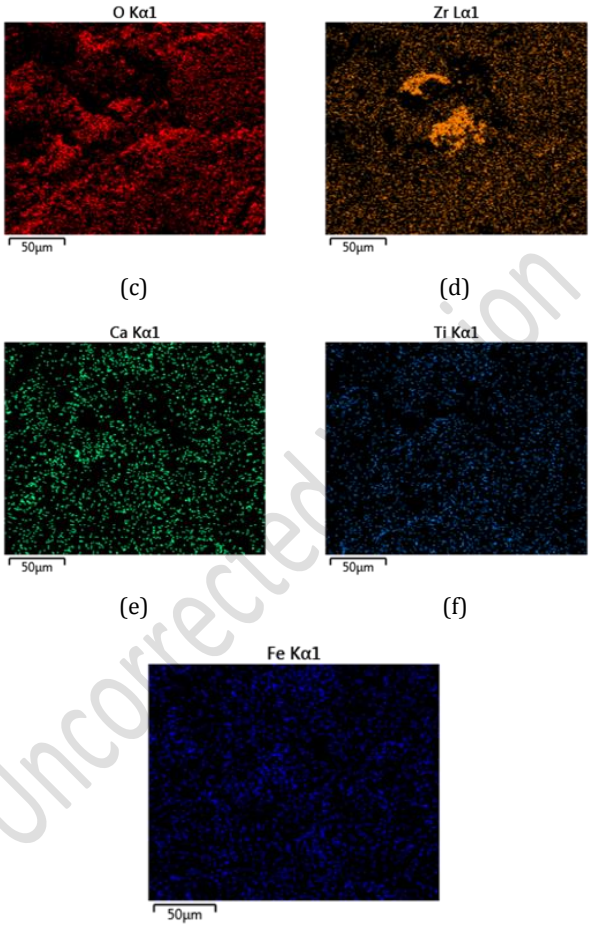

(c) (d) (e) (f) (g)

Figure 16. Mapping analysis of the Z1 material a) Si, b) Al, c) O, d) Zr, e) Ca, f) Ti and g) Fe

EDX-mapping results indicate that (Figure 10, Figure 12, Figure 14 and Figure 16), with the addition of waste input, the elemental composition of the chamotte refractory shows a slight decrease in Al content compared to chamotte refractory produced without additives. Conversely, there is a slight increase in Fe and Ti content, along with an increase in Zr content due to the waste addition. The highest Zr content is observed in material from the X coded waste, which, according to XRF analysis, contains the highest amount of ZrO_2 in its structure.

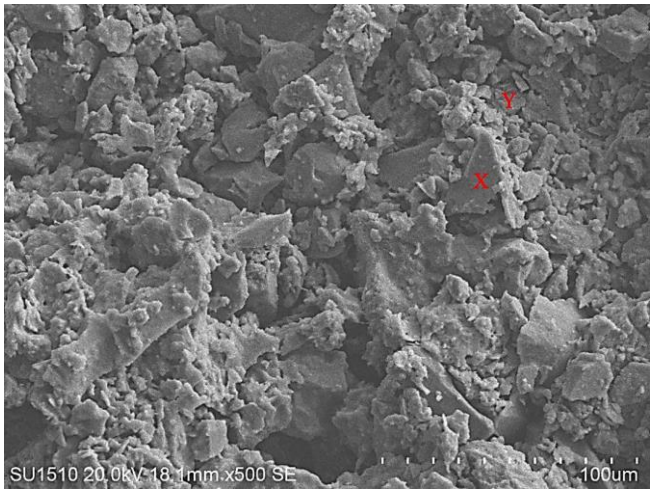

(a)

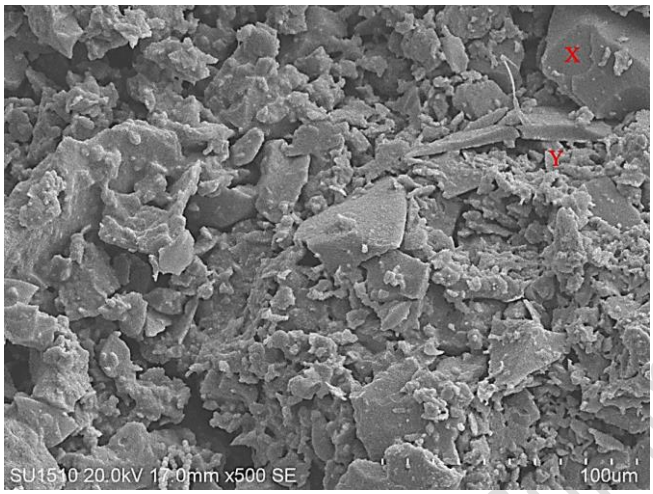

(b)

Figure 17. Fractured surface analysis of the reference material (X: intragranular Y: intergranular)

When analyzing the fracture surface images of the reference material before and after thermal shock (Figure 17), Examination of the fracture surface images of the material without additives, both before and after thermal shock, revealed that intergranular fractures were predominant in smaller grains, while intragranular fractures were dominant in larger grains.

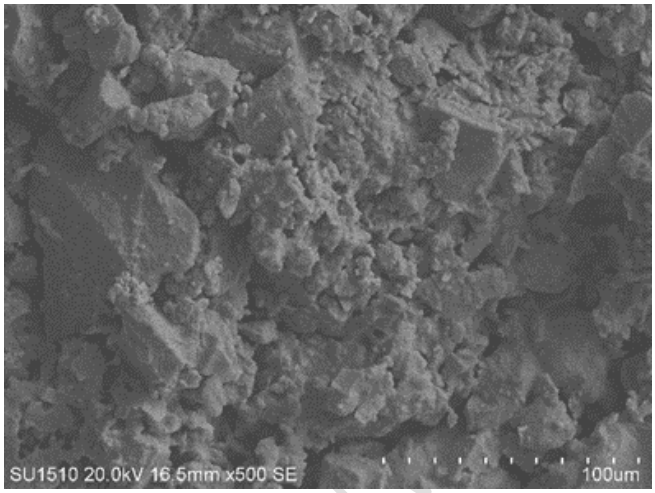

(a)

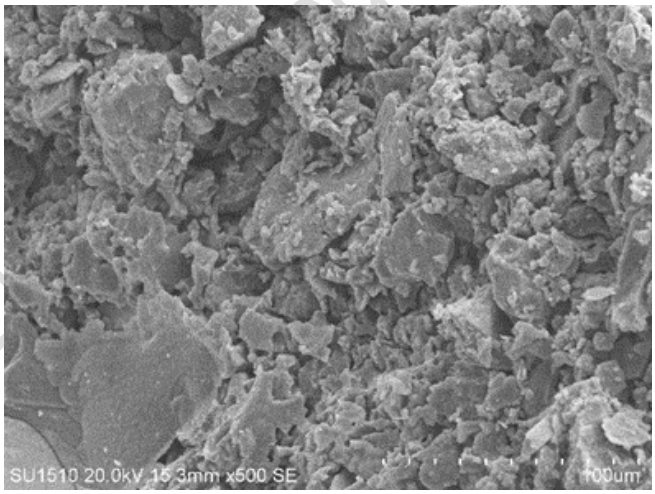

(b)

Figure 18. Fractured surface analysis of the X2 material

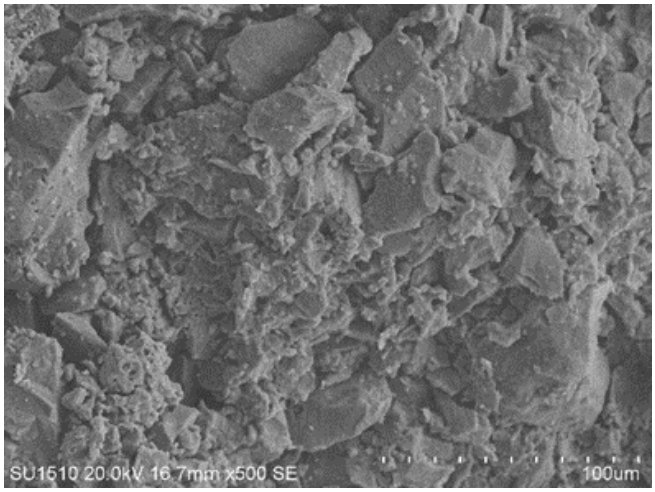

(a)

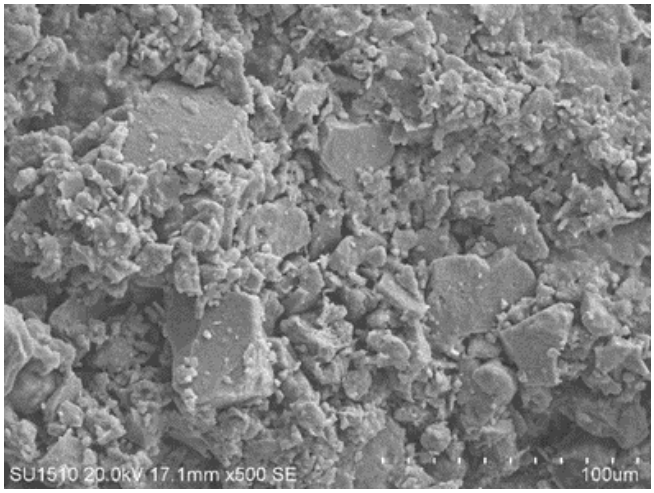

(b)

Figure 19. Fractured surface analysis of the Y2 material

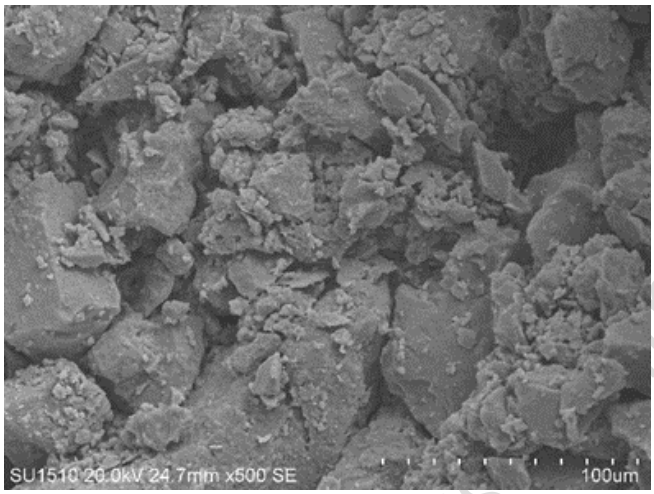

(a)

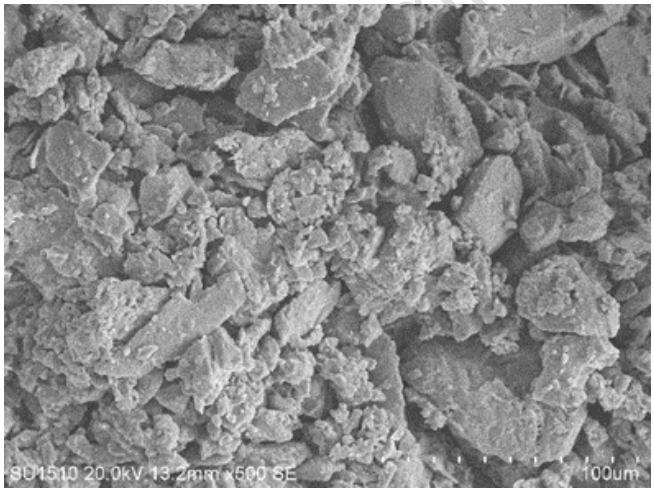

(b)

Figure 20. Fractured surface analysis of the Z1 material

As seen in Figures 18, Figure 19 and Figure 20, thermal shock before and after fracture surface images of X2, Y2, and Z1 coded high-alumina castable refractories are provided. Before thermal shock, intragranular fractures were more predominant. As intragranular fractures require higher energy, the addition of high-alumina PCWS supports the increase in mechanical properties, as evidence by the fracture surface images. After thermal shock, intergranular fractures were observed in small grains, while intragranular fractures were dominantly observed in large grains. It was believed that this change in fracture type supports the high strength rate after thermal shock. In the case of Z added refractory, in addition to predominantly intragranular fractures before thermal shock, deep cracks in the grains were also observed. After thermal shock, intragranular cracks were still present. It was observed that the amount of intragranular cracks increased from X-coded material to Z-coded material.

4 Conclusions

When the open porosity and density values of the produced refractory materials were examined, it was observed that the density of the X1, X2, Y1, Y2, and Z1 refractory types exceeded the density of the reference material. However, when the additive content exceeds a certain threshold, the density decreases compared to the reference material.

The decrease in mechanical properties after thermal shock has been associated with the formation of cracks. Compositional analysis by examining the fractured surfaces of the pristine material before and after thermal shock elucidates this relationship. In general, it was observed that the mechanical properties of all compositions decreased after thermal shock. This situation is caused by pre-existing cracks and newly formed cracks after thermal shock.

Compared to the additive-free fireclay refractory, samples containing X2, Y2, and Z1 precision-casting waste sand (PCWS) showed increases in 3-point bending strength by 27%, 10%, and 5%, respectively, after undergoing thermal shock testing. Similarly, with the addition of PCWS, X2 and Y2 samples exhibited increases of 17% and 33% in cold crushing strength (CCS) values.

Fractured surface analysis indicates that intergranular fractures dominate in small-sized grains, whereas intragranular fractures are common in larger grains. After thermal shock, intergranular cracks continued in small grains, while intragranular fractures were clearly dominant in large grains. This observation supports the conclusion that the strength rate after thermal shock remains relatively high.

An increase in the amount of intragranular cracks was observed after thermal shock. This increase from material coded as X to material coded as Z demonstrates that the addition of X2 results in the formation of few and short microcracks in the structure. These microcracks contribute to the overall durability of the material.

Microcracks resulting from the mismatch in thermal expansion coefficients also contribute to durability. However, the addition of increased waste leads to the formation of more microcracks, which contribute to the formation of larger cracks. This phenomenon has been shown to decrease the physical and mechanical properties of the material.

5 Acknowledgement

6 Author(s) Contribution Form

In the study carried out, Author 1 included the titles of literature review, evaluation of the obtained results, examination of the results and writing; Author 2 contributed to the formation of the idea, making the design, obtaining the materials used, and checking the article in terms of spelling.

7 Ethics committee approval and conflict of interest statement

"There is no need to obtain ethics committee permission for the article prepared."

"There is no conflict of interest with any person/institution in the article prepared."

8 References

[1] Yan J, Dai Y, Yan W, Jin S, Wang X, Li Y. "Effect of microporous aggregates and spinel powder on fracture behavior of magnesia-based refractories". Journal of the European Ceramic Society, 42(16), 7648-7655, 2022.

[2] Zhou W, Yan W, Ma S, Schafföner S, Dai Y, Li Y. "Degradation mechanisms of periclase-magnesium aluminate spinel refractory bricks used in the upper transition zone of a cement rotary kiln". Construction and Building Materials, 272, 121617, 2021.

[3] Dai Y, Li Y, Jin S, Harmuth H, Xu X. "Fracture behavior of magnesia refractory materials under combined cyclic thermal shock and mechanical loading conditions". Journal of the American Ceramic Society, 103, 1956-1969, 2020.

[4] Gruber D, Sistaninia M, Fasching C, Kolednik O. "Thermal shock resistance of magnesia spinel refractories—Investigation with the concept of configurational forces". Journal of the European Ceramic Society, 36(16), 4301-4308, 2016.

[5] Andrews A, Nsiah-Baafi E, Gawu S.K.Y., Olubambi P.A. "Synthesis of high alumina refractories from lithomargic clay". Ceramics International, 40(4), 6071-6075, 2014.

[6] Andrews A, Adam J, Gawu S.K.Y. Development of fireclay aluminosilicate refractory from lithomargic clay deposits. Ceramics International, 39(1), 779-783, 2013.

[7] American Society for Testing and Materials. "Standard Classification of Fireclay and High-Alumina Refractory Brick". https://www.astm.org/c0027-98r18.html (10.12.2021).

[8] Francois C. *Materials Handbook*, Springer, London, 2008.

[9] Hossain SkS, Roy P.K. "Sustainable ceramics derived from solid wastes: a review". Journal of Asian Ceramic Societies, 8(4), 984-1009, 2020.

[10] Lingling X, Wei G, Tao W, Nanru Y. "Study on fired bricks with replacing clay by fly ash in high volume ratio". Construction and Building Materials, 19(3), 243-247, 2005.

[11] Mahapatra MK. "Review of corrosion of refractory in gaseous environment". International Journal of Applied Ceramic Technology, 17(2), 606-615, 2020.

[12] Krishnan M, Manikandan R, Thenmuhil D. "Effect of heat treatment and zircon addition on the properties of low-cement castables based on recycled alumina grog". Ceramics International, 47(3), 3430-3443, 2021.

[13] Suchanek W.L. "Hydrothermal Synthesis of Alpha Alumina (α-Al_2O_3) Powders: Study of the Processing Variables and Growth Mechanisms". Journal of the American Ceramic Society, 93(2), 399-412, 2010.

[14] Xu X, Li J, Wu J, Tang Z, Chen L, Li Y, Lu C. "Preparation and thermal shock resistance of corundum-mullite composite ceramics from andalusite". Ceramics International, 43(2), 1762-1767, 2017.

[15] Zhang FC, Luo HH, Roberts SG. "Mechanical properties and microstructure of Al_2O_3/mullite composite". Journal of Materials Science, 42, 6798-6802, 2007.

[16] Zhao H, Ye C, Fan Z. "A simple and effective method for gel casting of zirconia green bodies using phenolic resin as a binder". Journal of the European Ceramic Society, 34(5), 1457-1463, 2014.

[17] Leo S, Tallon C, Stone N, Franks GV. "Near-Net-Shaping Methods for Ceramic Elements of (Body) Armor Systems". Journal of the American Ceramic Society, 97(10), 3013-3033, 2014.

[18] Sereni JGR. *Reference module in materials science and materials engineering*, 2016.

[19] Xiang R, Li Y, Li S, Xue Z, He Z, Ouyang S, Xu N. "The potential usage of waste foundry sand from investment casting in refractory industry", Journal of Cleaner Production, 211, 1322-1327, 2019.

[20] Avcıoğlu C, Bekheet MF, Artır R. "Radiation shielding and mechanical properties of mullite-zirconia composites fabricated from investment-casting shell waste". Journal of Materials Research and Technology, 24, 5883-5895, 2023.

[21] Reinhart TJ, Brinson HF. *Engineered Materials Handbook: Ceramics and glasses*. USA, ASM International, 1991.

[22] Özdemir S. Recycling of investment casting shell mold sands in ceramic industry. Master Thesis, Marmara Üniversitesi, Istanbul, Türkiye, 2013.

[23] Erdem Y. Hassas Döküm Atık Kumunun, Duvar Karosu, Porselen Karo ve Opak Sır Üretiminde Kullanımının Araştırılması. Doctoral Thesis, Necmettin Erbakan Üniversitesi, Konya, Türkiye, 2023.

[24] Avcıoğlu C. Reuse of Spent Investment Casting Foundry Sands in the Production of Structural Ceramics. Doctoral Thesis, Marmara Üniversitesi, Istanbul, Türkiye, 2023.

[25] Jigao L, Yuan-cai L, Tan S. "Experimental study on separation of valuable refractory aggregate from investment casting ceramic shell waste". China Foundry, 13(4), 243-247, 2016.

[26] Li J, Li Y, Wang L. "Study on technology of iron removal during recycling of shell of investment casting". Advanced Materials Research, 634-638, 3181-3184, 2013.

[27] British Standard. (1989). British standard testing of engineering ceramics BS 7134 British Standards Institution.

[28] Aksel, C. "The effect of mullite on the mechanical properties and thermal shock behaviour of alumina-mullite refractory materials". Ceramics International, 29, 183–188, 2003.

[29] Ceylantekin R, Aksel C. "MgO-Spinel kompozit refrakterlere ZrSiO4 ilavesinin korozyon davranışına etkisi". Anadolu Üniversitesi Bilim ve Teknoloji Dergisi-A Uygulamalı Bilim ve Mühendislik, 11, 103-114, 2010.

[30] Meng W, Ma C, Ge T, Zhong X. "Effect of zircon addition on the physical properties and coatability adherence of MgO–$2CaO{\cdot}SiO_2$–$3CaO{\cdot}SiO_2$ refractory materials". Ceramics International, 42(7), 9032-9037, 2016.

[31] Xiang R, Li Y, Li S, Ma X, Li Y, Sang S. "Effect of zircon content on the microstructure and physical properties of

chamotte refractories". Key Engineering Materials, 697, 604-607, 2016.
[32] Bahtli T, Bostanci VM. "Effect of precision casting sand waste of 4140 steel on the sintering and densification behaviour of chamotte refractories". Journal of Thermal Analysis and Calorimetry, 142, 2385-2390, 2020.
[33] Biswas N, Chaudhuri S. "Comparative study of zirconia-mullite and alumina-zirconia composites". Bulletin of Materials Science,; 22, 37-47, 1999.
[34] Chandra D, Das GC, Sengupta U, Maitra S. "Studies on the reaction sintered zirconia-mullite-alumina composites with titania as additive". Ceramica, 59(351), 487-494, 2013.
[35] Aksel C, Aksoy T. "Improvements on the thermal shock behaviour of MgO-spinel composite refractories by incorporation of zircon-3 mol% Y_2O_3". Ceramics International, 38(5), 3673-3681, 2012.
[36] Lin SK, Wu CH. "Improvement of Bond Strength and Durability of Recycled Aggregate Concrete Incorporating High Volume Blast Furnace Slag". Materials (Basel), 14(13), 3708, 2021.
[37] Bahtli T, Aksel C. "Thermal Shock Behaviour of Magnesia–Hercynite-Spinel Composite Refractories". Journal of Multidisciplinary Engineering Science and Technology, 3(6), 5083-5088, 2016.
[38] Dana K, Sinhamahapatra S, Tripathi HS, Ghosh A. "Refractories of alumina-silica system". Transactions of the Indian Ceramic Society, 73, 1–13, 2014.
[39] Liu KC, Thomas G, Caballero A, Moya JS, De Aza S. "Mullite formation in kaolinite-α-alumina". Acta Metallurgica et Materialia, 42, 489–495, 1994.
[40] Köksal NS, Ünlü BS, Meriç C. "Alümina esaslı refrakter tuğlaların ısıl şok davranışlarının incelenmesi". Pamukkale Üniversitesi Mühendislik Bilimleri Dergisi, 9(2), 147-151, 2003.
[41] Başpınar MS. Mullit refrakterlerde bağlayıcı fazın optimizasyonu. Doktora tezi, Anadolu Üniversitesi, Eskişehir, Türkiye, 2005.
[42] Bahtli T, Bostanci VM. "Paslanmaz çeliklerin hassas döküm kumu atıklarının katılmasıyla üretilen beyaz ergimiş alümina refrakterlerinin mekanik özellikleri ve termal şok dayanımları". Afyon Kocatepe Üniversitesi Fen ve Mühendislik Bilim Dergisi, 19, 440–446, 2019.